Blocking the PD-1-PD-L1 axis by a novel PD-1 specific nanobody expressed in yeast as a potential therapeutic for immunotherapy

Zongshu Xian [a, 1], Linlin Ma [b, 1], Min Zhu [c], Guanghui Li [c], Junwei Gai [c], Qing Chang [b], Yuliang Huang [a], Dianwen Ju [a, **], Yakun Wan [c, *]

[a] School of Pharmacy, Fudan University, Shanghai, China
[b] Jiading Distinct Central Hospital Affiliated Shanghai University of Medicine and Health Sciences, Shanghai, China
[c] Shanghai Novamab Biopharmaceuticals Co., Ltd., Shanghai, China

ARTICLE INFO

ABSTRACT

PD-1/PD-L1 pathway blocking with antibodies offers a vital and efficient therapeutic strategy to restore T cell-associated antitumor immunity and treats a variety of cancers in clinic. Nanobodies (Nbs) give several advantages over conventional monoclonal antibodies such as size, solubility, stability and costs. Additionally, *P. pastoris* is a suitable host for Nb production. Herein, we aim to produce and evaluate anti-PD-1 Nb derived from the *P. pastoris*. Our findings indicated that we successfully established the Nbs phage-displayed library against PD-1 with qualified library capacity and insert ratio. Anti-PD-1 Nb Nb97 was screened through PE-ELISA and flow cytometry. To extend half-life of Nb97, we contracted pPICZαA-Nb97-Nb97-HSA recombination vector, which was then transformed into the system of *P. pastoris* X-33. The yield of purified Nb97—Nb97-Human serum albumin (HSA) fused protein (MY2935) reached to 2.3 g/L after 147 h of fermentation. Meanwhile, the blocking effect of MY2935 is similar to that of MY2626 (humanized Nb97-Fc), and MY2935 showed better performance on stimulating the immune function through PD-1 reporter assay. Hence, *P. pastoris* X-33 expressing and secreting functional anti-PD-1 Nb-HSA fusion protein might be a system of high yield and low cost.

© 2019 Published by Elsevier Inc.

1. Introduction

Cancer immunotherapy is revolutionizing cancer treatment. Immunological checkpoint inhibitors are the most successful agents of cancer immunotherapy [1,2]. Programmed death 1 (PD-1), a pivotal immunosuppressed receptor appeared in T lymphocytes, mediates immunosuppression by recognizing the programmed death-ligand-1 (PD-L1) that is mainly expressed in tumors [3]. Accordingly, inhibition of PD-1/PD-L1 signal pathway is widely known as a revolutionary treatment against a multiple of malignant tumors. FDA has approved several monoclonal antibodies blocking PD-1 or PD-L1 include Nivolumab (PD-1, BMS), Atezolizumab (PD-L1, Roche), Pembrolizumab (PD-1, Merck), Durvalumab (PD-L1, AZ), and Avelumab (PD-L1, Merck) which show encouraging results for several malignancies with the overall response rate of about 10%—45% [4—8].

Nanobody (Nb) was derived from camelid heavy-chain antibodies, which is consisted of a single monomeric variable region [9]. Compared to common antibodies (about 150 kd), the size of Nb with 12—15 kd is much small. This low molecular mass gives many advantages to Nbs, such as high tissue permeability, high stability, high solubility and low aggregation propensity and easy cloning [10—13]. Recently, the European Medicines Agency has approved first Nb Cablivi for treating acquired thrombotic thrombocytopenic purpura in adults [14]. Therefore, Nbs are ideal tools to develop novel biological drugs with multiple competitive advantages over common antibodies or other therapeutic molecules. In this study, a

functional anti-PD-1 Nb Nb97 was screened by phage display technology derived from a camel immunized library with recombinant PD-1 antigen.

Yeast expression system has been widely used for the production of heterologous eukaryotic protein [15]. The major advantages of this system include high yield and productivity, lower protein production cost and mammalian-like proteins [16]. *Pichia pastoris* (*P. pastoris*), the methylotrophic yeast, is one of yeast strains widely applied in fermentation industry because *P. pastoris* is rapidly grown to high densities and has a strong promoter to enhance exogenous genes expression [17]. As eukaryotic systems, *P. pastoris* are also able to produce soluble, correctly folded recombinant proteins [18]. Thus, the recombinant proteins or antibody fragments obtained from *P. pastoris* are much suitable for therapeutic use [19—22].

In order to raise the production, serum half-life and inhibitory activities of Nb97, in the present research, Nb97—Nb97-Human serum albumin (HSA) fusion protein was produced in an expression system of *P. pastoris* X-33. The activity of Nb97 expressed in *P. pastoris* X33 system and the mammalian cell HEK 293F system was compared.

2. Material and methods

2.1. Cells

The HEK 293F, HEK 293T, A549 cells were obtained from the American Type Culture Collection (ATCC). GS-J2/PD-1 cells were purchased from Genscript company, China. TG1 cells and WK6 cells were kindly provided by Prof. Serge Muyldermans (Laboratory of Cellular and Molecular Immunology, VUB-Vrije Universiteit, Brussel, Belgium).

2.2. Bactrian camel immunization and Nb library construction

A healthy young Bactrian camel (*Camelus bactrianus*) was first immunized using the mixture of recombined PD-1-Fc protein [23] and Freund's complete adjuvant (Sigma-Aldrich, StLouis, MO, USA), and then continued to accept immunization with Freund's incomplete adjuvant (Sigma-Aldrich) for six times. After the seventh immunization, peripheral blood lymphocytes (PBLs) were harvested from camel blood. All procedures were conducted according to the standard operating procedure approved by the Institutional Animal Ethics Committee.

Total RNA was isolated from PBLs with the RNA extraction kit (QIAGEN, Germantown, MD, USA), and the cDNA was synthesized through reverse transcription PCR with a Super-Script III FIRST STRAND SUPERMIX KIT (Invitrogen, Carlsbad, California, USA). Then VHH was amplified with nested PCR according to the following primers: Forward-1: GTCCTGGCTGCTCTTCTACAAGGC; Reverse-1: GGTACGTGCTGTTGAACTGTTCC; Forward-2: GATGTGCAGCTGCAG-GAGTCTGGRGGAGG; Reverse-2: GGACTAGTGCGGCCGCTGGA-GACGGTGACCTGGGT. The final product was digested by *Pst* I and *Not* I and then inserted into the pMECS vector, which was then transformed into *E.coli* TG1 cells. The library size was evaluated by plating transformants on solid 2×tryptone and yeast (TY) medium supplemented with 100 μg/mL ampicillin and 2% glucose, and the number of colonies were measured after a gradient dilution. In addition, the insertion rate was detected with PCR amplification.

2.3. Screening of PD-1-specific Nbs by phage display technology

The anti-PD-1 VHHs were screened on PD-1-Fc coated proteins and then enriched by bio-panning for consecutive rounds, with the infection of VCSM13 helper phages. Briefly, 500 μL library stock was grown in 2×TY medium supplementing 1% glucose, 70 μg mL^{-1} kanamycin and 100 μg mL^{-1} ampicillin for 2.5 h at 37 °C, then 1×10^{12} VCSM13 helper phages were added to the medium. After incubating at 25 °C for 30 min, the infected cells were collected by centrifugation and resuspended into 2×TY medium with kanamycin and ampicillin. The library of VHHs was displayed on the phages after incubating at 37 °C overnight. The phages were further precipitated by PEG/NaCl and then resuspended with PBS. Thereafter, 2×10^{11} phages were used for selecting on immobilized PD-1-Fc coated 96-well microtiter plates. Phages expressing anti-PD-1 VHHs were enriched through several rounds of bio-panning.

2.4. Periplasmic extract ELISA (PE-ELISA)

In order to get positive clones, 96 clones were selected randomly through PE-ELISA. Each selected clone was cultured in 1 mL Terrific Broth medium (TB) (Invitrogen) containing ampicillin for 3 h and induced by 1 mM IPTG overnight. After an osmotic shock, the cell supernatants were collected and transferred into the microtiter plate wells coated with PD-1-Fc or Fc in advance. 1 h later, the mouse anti-HA antibody as well as goat anti-mouse IgG-alkaline phosphatase were used and incubated successively. Then, 405 nm absorbance was read by the microplate reader (Bio-Rad, Hercules, CA, USA) after the substrate of alkaline phosphatase was added. At last, the selected positive clones were divided into different families according to the sequence of amino acids in the complementary determining region 3 (CDR3).

2.5. Screening of PD-1/PD-L1 interaction blocking Nb through flow cytometry

The HEK 293T-PD-1 stable cell line was constructed using a lentiviral packaging system. 1×10^7 HEK 293T-PD-1 cells resuspended in PBS (0.5% BSA) buffer were transferred in 96-well plates, then 2 μg candidate anti-PD-1 Nbs were added to the wells with control Nb as isotype antibody control. Meanwhile, HEK 293T cells was used as negative cell control. All samples were incubated with 0.3 μg PD-L1-Fc-Biotin for 0.5 h. The samples were then stained with SA-PE (eBioscience, San Diego, CA, USA). Then the ratio of Nbs interrupting the interaction between PD-1 and PD-L1 was determined with flow cytometry (BD Biosciences, San Jose, CA, USA).

2.6. Expression of anti-PD-1 Nb through microbial expression purification system

The *HSA* sequence (Accession number: NP_000468.1) was amplified from the cDNA library from A549 cell line, and linked it to two replicated sequences of anti-PD-1 Nb. Next, the fused fragment was ligated into linearized pPICZαA vector, and then the recombinant vector was transformed into *P. pastoris* X-33 competent cells by electroporation. The positive transformants including anti-PD-1 Nb-HSA fused protein expression cassettes were identified by SDS-PAGE analysis.

2.7. Condition optimization of induced protein expression

A single colony including Nb-HSA fused protein expression cassettes was transformed into buffered complex glycerol (BMGY) medium and incubated at 28 °C for 24 h. Then the protein was cultured in shake flask on an extended scale. In order to obtain anti-PD-1 Nb-HSA with the optimal quality and quantity, the culture conditions were optimized through setting down different inducing factors, including the induction temperature, PH value and methanol concentration.

2.8. Nb purification and quantitative determination

When anti-PD-1 Nb-HSA was induced in BIOTECH-7BG fermentation tank (Shanghai baoxing biological equipment engineering co., LTD, China), the dissolved oxygen (DO) was maintained at 25% by supplementing glycerol and methanol, the protein titers and wet cell weights were detected at different times.

Furthermore, the Nb was purified through Capto™ Blue (GE Healthcare, Madison, WI, USA) and Superdex 200 Increase GL columns (GE Healthcare) on ÄKTA pure 150 (GE Healthcare) successively. Ultimately the purity of the purified Nb was determined by HPLC analysis using Waters Acquity UPLC™ system with XBridge Protein BEH SEC 200 Columns (Waters Corporation, Milford, MA, USA).

2.9. Neutralization assay

The 50% inhibitory concentration (IC_{50}) were determined by flow cytometry. Briefly, HEK 293T cells stably expressing PD-1 were incubated with diluted anti-PD-1 Nb and PD-L1-Fc-Biotin. Then cells were wash with PBS (0.1% Tween) and stained by SA-PE. Finally, the mean fluorescence intensities (MFI) were measured.

2.10. PD-1 reporter assay

The functional evaluation assay of anti-PD-1 antibodies was purchased from Genscript company, China. Briefly, GS-J2/PD-1 cells were grown in F12K complete medium containing 10% FBS (Gibco, GrandIsland, NY, USA) as well as 1% Penicillin-Streptomycin (Invitrogen). 20 μL GS-J2/PD-1 cells were added to 384 wells plates (1.25×10^4 per well) and incubated with anti-PD-1 antibodies for 6 h at 37 °C. Then ONE-Glo™ Luciferase reagent was added and the

firefly luminescence was then determined after 5–10 min on Bio-TeK plate reader (Biotek Instruments, Inc., Vermont, USA). Finally, the 50% effective concentration (EC_{50}) of antibodies was determined.

2.11. Statistical analyses

Statistical analyses were performed through GraphPad Prism 6.0. Results are expressed as mean ± SD.

3. Results

3.1. The construction of immunized anti-PD-1 Nb phage library

The schematic illustration of strategies to construct anti-PD-1 Nb phage library and select the PD-1 specific VHHs was displayed in Fig. 1A. As shown in Fig. 1B, PD-1 ectodomain fused to Fc (PD-1-ECD-Fc) was purified through eukaryotic expression system with high purity, which was used as antigen to immunize a young healthy Bactrian camel for 7 times. After the final immunization, total RNA was extracted from PBLs of PD-1-immunized Bactrian camels. The VHHs gene encoding fragments were amplified through a nest PCR amplification which includes a primary PCR for producing 700 bp fragments of VHH-h-CH2 and a second PCR for generating 400 bp fragments of VHH (Fig. 1C). After electrotransforming the recombinant pMECS-VHH vector into TG1 cells, the library capacity and insert ratio were determined. As shown in Fig. 1D, the diluted library cultured on the plates indicated a total size of 2.1×10^9 colony-forming units (CFU). Meanwhile, the results of PCR indicated that 91% clones have been correctly inserted (Fig. 1E). Collectively, the findings suggested that we successfully constructed a phage-displayed Nbs library targeting PD-1.
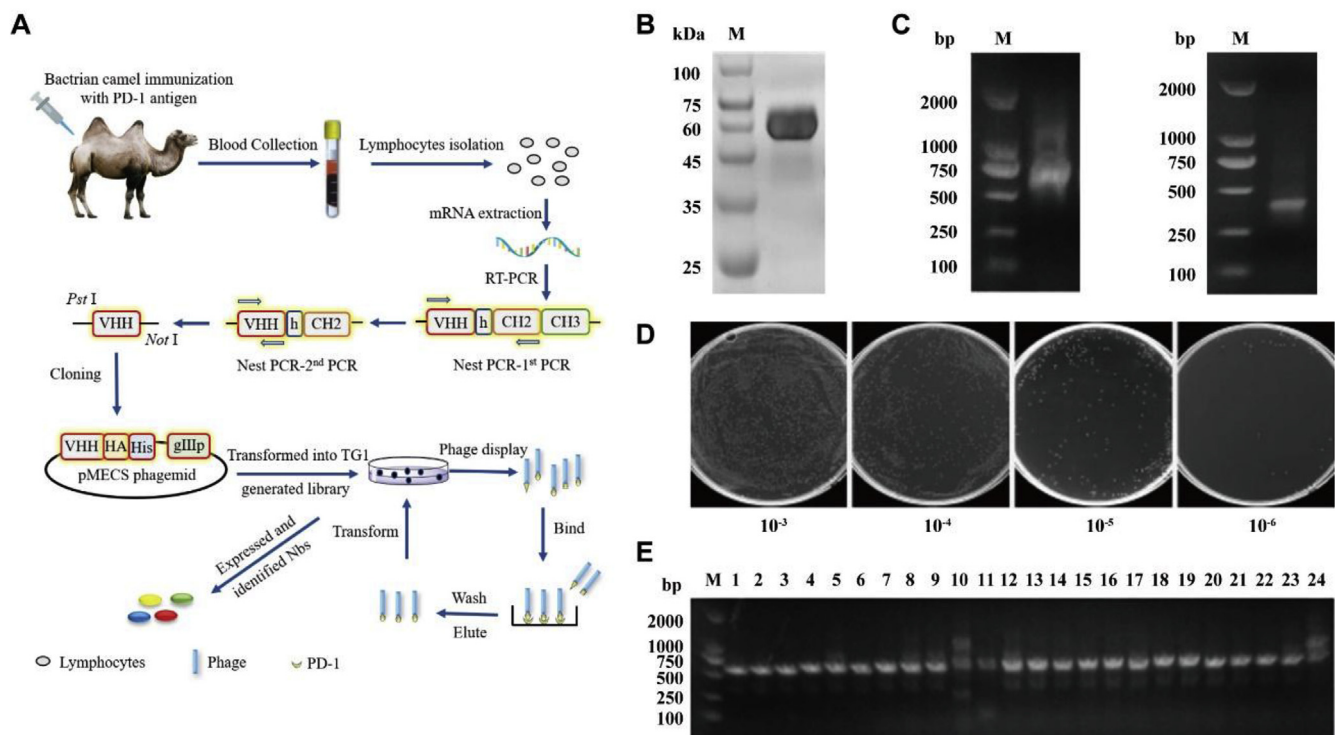

Fig. 1. Construction of anti-PD-1 Nbs phage-displayed library. (A) Schematic illustration of strategies to select the PD-1-specific VHHs. (B) The expression of PD-1-ECD-Fc was detected by SDS-PAGE. (C) The segments containing VHH gene fragments were amplified by a first PCR (left) and a second, nested PCR (right). (D) The capacity of the libraries was determined by counting the number of clones on plates after gradient dilution. (E) The correct insertion rate of library was estimated by performing PCR on randomly selected 24 colonies.

3.2. Selection of PD-1-specific Nbs

To screen PD-1-specific Nbs, four consecutive rounds of bio-panning using PD-1-Fc as antigen were performed through phage display, after which the enrichment fold of PD-1-specific VHHs has been reached to 21.3 times (Fig. 2A). In addition, 53 positive clones with a binding ratio >3 were identified from a total of 96 random clones by PE-ELISA assay (Fig. 2B), and sequencing analysis revealed that Nbs were divided into 6 groups based on the difference of amino acid in CDR3 (data not shown). Thereafter, we transformed the VHH cloned in pMECS vector to WK6 cells to express nano-bodies. Finally, the blocking PD-1-specific Nbs were selected by flow cytometry, As indicated in Fig. 2C, anti-PD-1 Nb97 significantly interrupted the interaction between PD-1 and PD-L1 with the ratio of 50.1%, compared with anti-AF70 isotype antibody. Hence, Nb97 was selected as the candidate PD-1-specific functional Nb for further study.

3.3. Determination of the optimal inducing condition to express Nb97–Nb97-HSA recombinant protein in yeast expression system

In order to purify anti-PD-1 Nb through microbial expression system, we amplified the HSA sequence from the cDNA library from A549 cell line, and linked it to two replicated sequences of Nb97, with the purpose of prolonging the half-life time of Nb and enhancing the recognition action towards PD-1. Thereafter, the fused fragment was inserted into pPICZαA vector and transformed into the system of *P. pastoris* X-33 cells. As shown in Fig. 3A, the Nb97–Nb97-HSA recombinant protein was correctly expressed according to the SDS-PAGE analysis, and clone NO. 3 (MY2395) was selected for further induction experiment. As indicated in Fig. 3B–D, a series of different inducing conditions were setting down to determine the optimal condition of protein purification. The protein expression with the highest rates occurred at 28 °C, pH 6.4, concentration of 2% methanol.
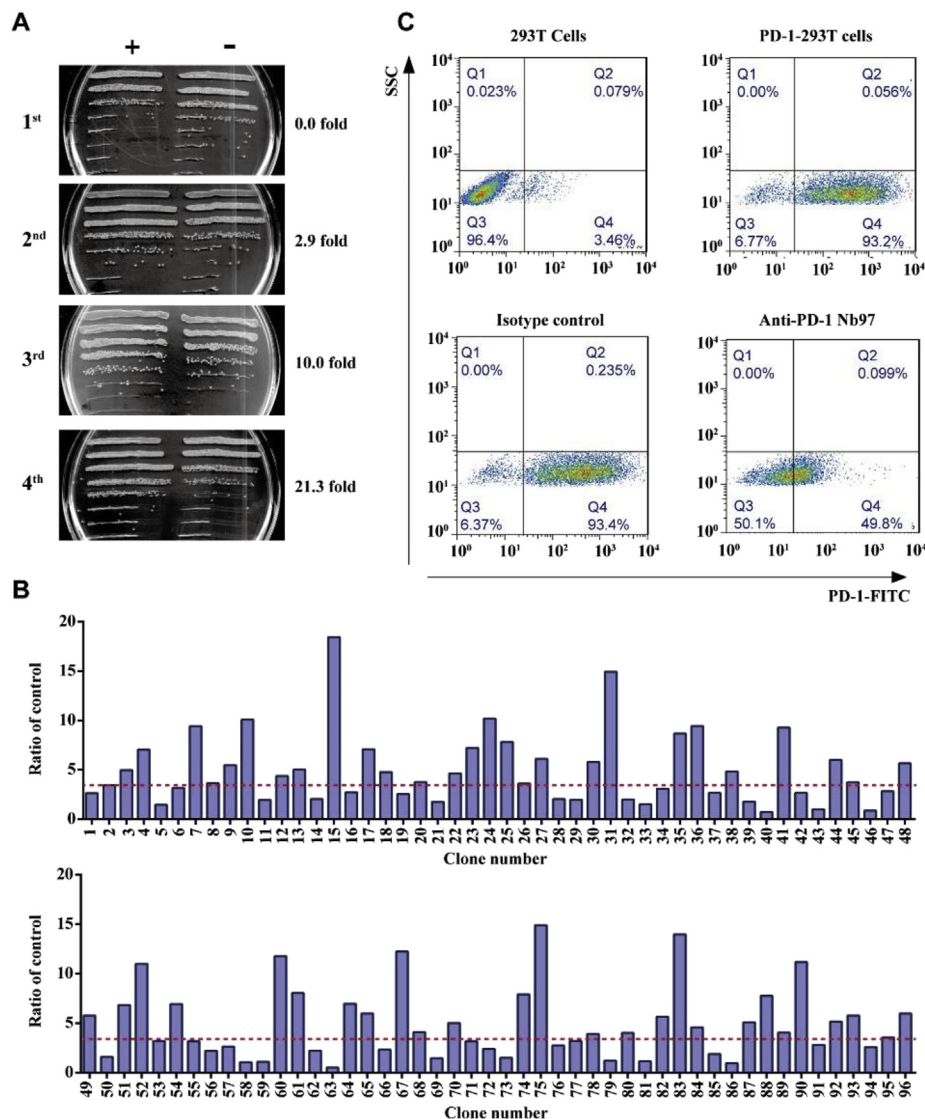

Fig. 2. PD-1-specific Nbs were selected from phage display library. (A) The enrichment for phage particles was detected after each round of panning. Phages collected from each round were incubated with PD-1-Fc or Fc coated on the wells, respectively. Then, the eluted phages were transformed into TG1 cells. +: Phages transformed into TG1 cells after panning with PD-1-Fc. −: Phages panning with Fc were used as control. (B) Periplasmic extract ELISA (PE-ELISA) was performed to identify positive clones. The ratio higher than 3 was considered as positive. (C) Blocking anti-PD-1 Nbs were screened through flow cytometry assay. The 293T-PD-1 stable cell was incubated with PD-L1-Fc-Biotin, and treated with candidate anti-PD-1 Nbs or anti-AF70 Nb simultaneously, 293T cells was used as negative cell control. The ratio of Nbs interrupting the interaction between PD-1 and PD-L1 was measured by flow cytometry.

After determining the optional induction condition, we further induced MY2395 in fermentation tank for large-scale fermentation, in which the dissolved oxygen (DO) was maintained at 25%. As shown in Fig. 3E–F, the total yields of recombinant protein obtained from *P. pastoris* was reached to 2.3 g/L approximately, and the optimal induction time was 147 h. In addition, after affinity chromatography and molecular sieve chromatography, the purity of Nb97–Nb97-HSA recombinant protein was 95.3% through HPLC analysis (Fig. 3G).

3.4. Comparison of the function between mammal cell derived and yeast derived anti-PD-1 Nbs

To compare the blocking effect of Nb derived from mammal cell and *P. pastoris*, neutralization assay was performed. Serial dilutions of MY2935 (expressed in *P. pastoris*) and MY2626 (humanized Nb97-Fc, expressed in mammal cells) were incubated with PD-1 stable-expressing cells in the presence of PD-L1-Fc protein. The result indicated that MY2935 had similar inhibitory effect against PD-1 compared to MY2626 (IC$_{50}$: 0.964 μg/mL vs 1.217 μg/mL) (Fig. 4A, Table 1).
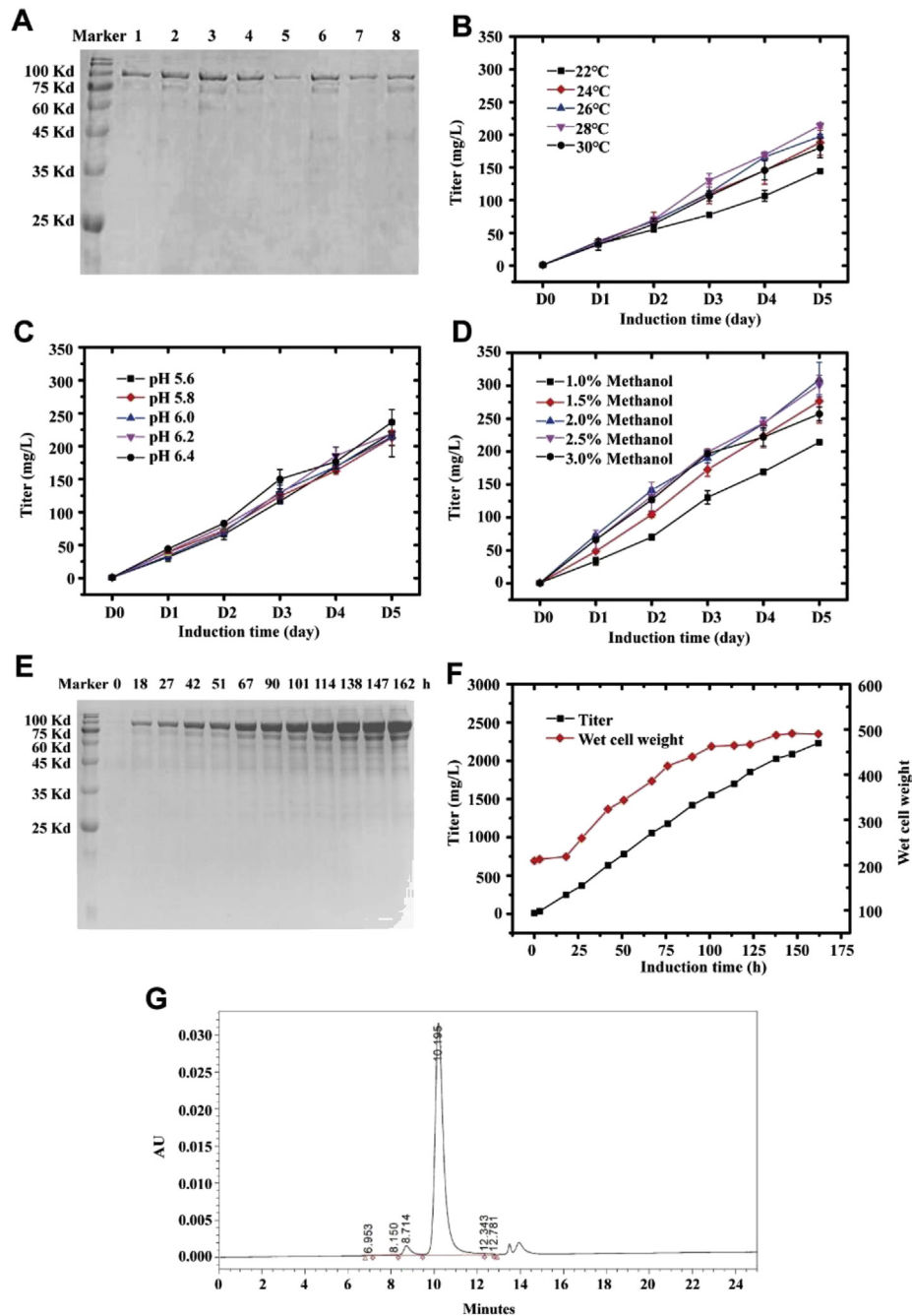
Fig. 3. Determination of the optimal inducing condition of Nb97–Nb97-HSA fused protein purified with microbial expression system. (A) The protein expressions of 8 selected clones was detected by SDS-PAGE analysis. (B–D) The effects of temperature, pH values and different methanol concentrations on Nb production. The results were displayed as titer (mg/L). (E–F) The yield of Nb in fermentation tank was detected at indicated times. The protein expressions were detected through SDS-PAGE assay (E), the protein titer and wet cell weight were both measured (F). (G)The purification of Nb was determined through HPLC analysis. The experiments were performed in triplicate.
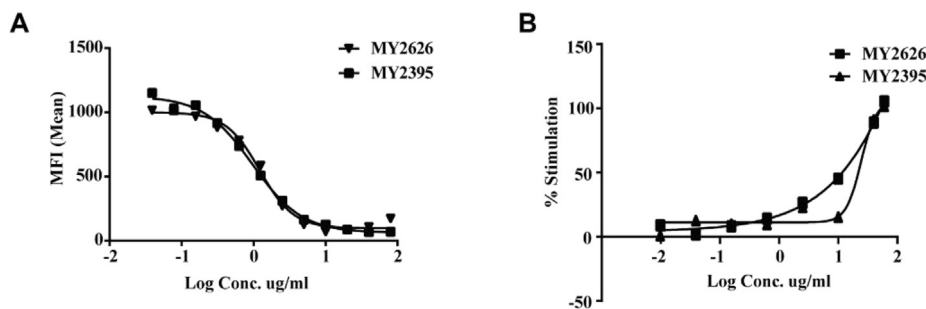
Fig. 4. Comparison of the function between mammal cell derived and yeast derived anti-PD-1 Nbs. (A) The blocking effect of Nbs towards the interaction between PD-1 and PD-L1 was detected by flow cytometry. MFI: median fluorescence intensity. (B) The immune stimulating effect of Nbs was determined by PD-1 reporter assay. The experiments were performed in triplicate. MY2626: Nb97-Fc produced in HEK 293F mammal cells and humanized. MY2395: Nb97–Nb97-HSA produced in *P. pastoris* yeast cells.

Table 1
Comparison of blocking effect and PD-1 reporter stimulation effect between MY2626 and MY2395.

	MY2626 ($\mu g/mL$)	MY2395 ($\mu g/mL$)
Blocking effect (IC_{50})	1.217	0.964
PD-1 reporter assay (EC_{50})	981.0	24.48

[a]IC_{50}: 50% inhibitory concentration.
[b]EC_{50}: 50% effective concentration.

For further comparing the immune stimulating effect between Nbs produced in mammal cell and *P. pastoris*, PD-1 reporter assay was performed. MY2935 exhibited better blockage effect towards PD-1/PD-L1 pathway than MY2626 (EC_{50}: 24.48 $\mu g/mL$ vs 981.0 $\mu g/mL$) (Fig. 4B, Table 1). Taken together, these results imply that anti-PD-1 Nb production in yeast expression system enhanced its quality and quantity, compared to the mammal cell expression system.

4. Discussion

The approved antibodies against PD-1 or PD-L1 show giant advantages in the treatment of cancer. However, they have a specific drawback that their large size is an obstacle for them into the interior of the tumor [24]. The additional limitation is that Fc-mediated effect may induce the undesirable depletion of the activated lymphocytes, resulting in the decreased anti-cancer immune response [25,26]. Nbs, characterized by small size and Fc fragment loss, represent an alternative strategy for the development of the agents targeting PD-1. In this study we obtained the smallest antibody fragment VHH (Nb) targeting PD-1. More importantly, anti-PD-1 Nb97–Nb97-HSA fusion protein MY2935 was obtained in the *P. pastoris* X-33 cells to extend half-life of anti-PD-1 Nb, which inhibited the interaction between PD-1 and PD-L1. Our results suggest that MY2935 deserves further development because it has the potential to be a better anti-PD-1 agent than existing monoclonal antibodies targeting PD-1.

Despite their advantage over monoclonal antibodies, small size of Nbs has the short serum half-life considering rapid clearance from bloodstream by renal elimination. Strategies for half-life extension of such Nb mainly involve binding to high-molecular weight carriers or permanent covalent conjugation that reduce the renal elimination rate [27,28]. HSA is an important carrier to extend half-life of small-size protein due to its availability, biocompatibility, low toxicity, and minimal to none immunogenicity [29]. Cancer cells usually have an increased albumin uptake, which provides the opportunities to drug distributing mainly into tumor cells through forming drug-albumin complexes [30,31]. In our study, we thus fused anti-PD-1 Nb to HSA to extend serum half-

life of this Nb. We obtained this fusion protein MY2935 using the expression system of *P. pastoris* X-33 cells transfected with pPICZαA-anti-PD-1-HSA fusion expression vector. In functional assay, this fusion protein MY2935 significantly inhibited the interaction between PD-1 and PD-L1, suggesting that MY2935 is a functional fusion protein. In the present study, we have not studied the serum half-life of MY2935 as well as its concentration in tumor. We will further explore this in future.

Monoclonal antibody is produced in mammalian cells, which has limitations in scaling up and long processing time, resulting in high cost. In contrast, Nb could be produced on a large scale in various systems including *Pichia pastoris*, *Saccharomyces cerevisiae* and *Escherichia coli*, of which *Pichia pastoris* is the most common expression system due to high cell densities, post-translation modification and easy to purification. In the present study, we successfully obtained MY2935 with the yield of 2.3 g/L after 147 h of fermentation in *P. pastoris* X-33. Importantly, blocking effect (IC_{50}) of MY2935 derived from *P. pastoris* X-33 is similar to that of MY2626 obtained from the mammalian cell HEK 293F. Taken together, compared with current mammalian expression system, expressing and secreting functional anti-PD-1 Nb-HSA fusion protein from *P. pastoris* X-33 might be a system with high yield and low cost.

Conflicts of interest

All commercial rights from this paper belong to Shanghai Novamab Biopharmaceuticals Co., Ltd.

Acknowledgements

References

[1] A.H. Sharpe, Introduction to checkpoint inhibitors and cancer immunotherapy, Immunol. Rev. 276 (2017) 5–8.
[2] R.A.M. Wilson, T.R.J. Evans, A.R. Fraser, R.J.B. Nibbs, Immune checkpoint inhibitors: new strategies to checkmate cancer, Clin. Exp. Immunol. 191 (2018) 133–148.
[3] J. Sunshine, J.M. Taube, PD-1/PD-L1 inhibitors, Curr. Opin. Pharmacol. 23 (2015) 32–38.
[4] L.J. Scott, Nivolumab: a review in advanced melanoma, Drugs 75 (2015) 1413–1424.
[5] K. Rihawi, F. Gelsomino, F. Sperandi, B. Melotti, M. Fiorentino, L. Casolari, A. Ardizzoni, Pembrolizumab in the treatment of metastatic non-small cell lung cancer: a review of current evidence, Ther. Adv. Respir. Dis. 11 (2017) 353–373.
[6] H.A. Blair, Atezolizumab: a review in previously treated advanced non-small

cell lung cancer, Target. Oncol. 13 (2018) 399–407.

[7] Y.M. Ning, D. Suzman, V.E. Maher, L. Zhang, S. Tang, T. Ricks, T. Palmby, W. Fu, Q. Liu, K.B. Goldberg, G. Kim, R. Pazdur, FDA approval summary: Atezolizumab for the treatment of patients with progressive advanced urothelial carcinoma after platinum-containing chemotherapy, The Oncologist 22 (2017) 743–749.

[8] S.J. Antonia, A. Villegas, D. Daniel, D. Vicente, S. Murakami, R. Hui, T. Yokoi, A. Chiappori, K.H. Lee, M. de Wit, B.C. Cho, M. Bourhaba, X. Quantin, T. Tokito, T. Mekhail, D. Planchard, Y.C. Kim, C.S. Karapetis, S. Hiret, G. Ostoros, K. Kubota, J.E. Gray, L. Paz-Ares, J. de Castro Carpeno, C. Wadsworth, G. Melillo, H. Jiang, Y. Huang, P.A. Dennis, M. Ozguroglu, P. Investigators, Durvalumab after chemoradiotherapy in stage III non-small-cell lung cancer, N. Engl. J. Med. 377 (2017) 1919–1929.

[9] S. Muyldermans, Nanobodies: natural single-domain antibodies, Annu. Rev. Biochem. 82 (2013) 775–797.

[10] S. Steeland, R.E. Vandenbroucke, C. Libert, Nanobodies as therapeutics: big opportunities for small antibodies, Drug Discov. Today 21 (2016) 1076–1113.

[11] M. Kijanka, B. Dorresteijn, S. Oliveira, P.M. van Bergen en Henegouwen, Nanobody-based cancer therapy of solid tumors, Nanomedicine 10 (2015) 161–174.

[12] S. Tabares-da Rosa, M. Rossotti, C. Carleiza, F. Carrion, O. Pritsch, K.C. Ahn, J.A. Last, B.D. Hammock, G. Gonzalez-Sapienza, Competitive selection from single domain antibody libraries allows isolation of high-affinity antihapten antibodies that are not favored in the llama immune response, Anal. Chem. 83 (2011) 7213–7220.

[13] J. Yan, G. Li, Y. Hu, W. Ou, Y. Wan, Construction of a synthetic phage-displayed Nanobody library with CDR3 regions randomized by trinucleotide cassettes for diagnostic applications, J. Transl. Med. 12 (2014) 343.

[14] S. Duggan, Caplacizumab: first global approval, Drugs 78 (2018) 1639–1642.

[15] D. Mattanovich, P. Branduardi, L. Dato, B. Gasser, M. Sauer, D. Porro, Recombinant protein production in yeasts, Methods Mol. Biol. 824 (2012) 329–358.

[16] J. Yin, G. Li, X. Ren, G. Herrler, Select what you need: a comparative evaluation of the advantages and limitations of frequently used expression systems for foreign genes, J. Biotechnol. 127 (2007) 335–347.

[17] V. Looser, B. Bruhlmann, F. Bumbak, C. Stenger, M. Costa, A. Camattari, D. Fotiadis, K. Kovar, Cultivation strategies to enhance productivity of Pichia pastoris: a review, Biotechnol. Adv. 33 (2015) 1177–1193.

[18] R. Baghban, S. Farajnia, Y. Ghasemi, M. Mortazavi, N. Zarghami, N. Samadi, New developments in Pichia pastoris expression system, review and update, Curr. Pharmaceut. Biotechnol. 19 (2018) 451–467.

[19] L.M. Emberson, A.J. Trivett, P.J. Blower, P.J. Nicholls, Expression of an anti-CD33 single-chain antibody by Pichia pastoris, J. Immunol. Methods 305 (2005) 135–151.

[20] S. Pourasadi, S.L. Mousavi Gargari, M. Rajabibazl, S. Nazarian, Efficient production of nanobodies against urease activity ofHelicobacter pylori in Pichia pastoris, Turk. J. Med. Sci. 47 (2017) 695–701.

[21] R. Baghban, S.L. Gargari, M. Rajabibazl, S. Nazarian, H. Bakherad, Camelid-derived heavy-chain nanobody against Clostridium botulinum neurotoxin E in Pichia pastoris, Biotechnol. Appl. Biochem. 63 (2016) 200–205.

[22] S. Ryckaert, E. Pardon, J. Steyaert, N. Callewaert, Isolation of antigen-binding camelid heavy chain antibody fragments (nanobodies) from an immune library displayed on the surface of Pichia pastoris, J. Biotechnol. 145 (2010) 93–98.

[23] B. Wan, H. Nie, A. Liu, G. Feng, D. He, R. Xu, Q. Zhang, C. Dong, J.Z. Zhang, Aberrant regulation of synovial T cell activation by soluble costimulatory molecules in rheumatoid arthritis, J. Immunol. 177 (2006) 8844–8850.

[24] C.M. Lee, I.F. Tannock, The distribution of the therapeutic monoclonal antibodies cetuximab and trastuzumab within solid tumors, BMC Canc. 10 (2010) 255.

[25] J.R. Brahmer, C.G. Drake, I. Wollner, J.D. Powderly, J. Picus, W.H. Sharfman, E. Stankevich, A. Pons, T.M. Salay, T.L. McMiller, M.M. Gilson, C. Wang, M. Selby, J.M. Taube, R. Anders, L. Chen, A.J. Korman, D.M. Pardoll, I. Lowy, S.L. Topalian, Phase I study of single-agent anti-programmed death-1 (MDX-1106) in refractory solid tumors: safety, clinical activity, pharmacodynamics, and immunologic correlates, J. Clin. Oncol. Off. J. Am. Soc. Clin. Oncol. 28 (2010) 3167–3175.

[26] R. Dahan, E. Sega, J. Engelhardt, M. Selby, A.J. Korman, J.V. Ravetch, FcgammaRs modulate the anti-tumor activity of antibodies targeting the PD-1/PD-L1 axis, Cancer Cell 28 (2015) 285–295.

[27] E.L. Schneider, B.R. Hearn, S.J. Pfaff, S.D. Fontaine, R. Reid, G.W. Ashley, S. Grabulovski, V. Strassberger, L. Vogt, T. Jung, D.V. Santi, Approach for half-life extension of small antibody fragments that does not affect tissue uptake, Bioconjug. Chem. 27 (2016) 2534–2539.

[28] R. Stork, E. Campigna, B. Robert, D. Muller, R.E. Kontermann, Biodistribution of a bispecific single-chain diabody and its half-life extended derivatives, J. Biol. Chem. 284 (2009) 25612–25619.

[29] K. Taguchi, V.T. Chuang, T. Maruyama, M. Otagiri, Pharmaceutical aspects of the recombinant human serum albumin dimer: structural characteristics, biological properties, and medical applications, J. Pharm. Sci. 101 (2012) 3033–3046.

[30] G.J. Quinlan, G.S. Martin, T.W. Evans, Albumin: biochemical properties and therapeutic potential, Hepatology 41 (2005) 1211–1219.

[31] B. Rogers, D. Dong, Z. Li, Z. Li, Recombinant human serum albumin fusion proteins and novel applications in drug delivery and therapy, Curr. Pharmaceut. Des. 21 (2015) 1899–1907.